



# Establishment and transcriptomic features of an immortalized hepatic cell line of the Chinese tree shrew

Xuemei Zhang<sup>1</sup> · Dandan Yu<sup>2</sup> · Yong Wu<sup>2</sup> · Tianle Gu<sup>2,3</sup> · Na Ma<sup>1</sup> · Shaozhong Dong<sup>1</sup> · Yong-Gang Yao<sup>2,3,4</sup>

Received: 19 June 2020 / Revised: 3 August 2020 / Accepted: 23 August 2020 / Published online: 3 September 2020  
© Springer-Verlag GmbH Germany, part of Springer Nature 2020

## Abstract

**Background** The Chinese tree shrew (*Tupaia belangeri chinesis*) is a rising experimental animal and has been used for studying a variety of human diseases, such as metabolic and viral infectious diseases.

**Methods** In this study, we established an immortalized tree shrew hepatic cell line, ITH6.1, by introducing the simian virus 40 large T antigen gene into primary tree shrew hepatocytes (PTHs).

**Results** The ITH6.1 cell line had a stable cell morphology and proliferation activity. This cell line could be infected by enterovirus 71 (EV71), but not hepatitis C virus (HCV), although the known HCV entry factors, including CD81, SR-BI, CLDN1 and OCLN, were all expressed in the PTHs and ITH6.1 of different passages. Comparison of the transcriptomic features of the PTHs and different passages of the ITH6.1 cells revealed the dynamic gene expression profiles during the transformation. We found that the DNA replication- and cell cycle-related genes were upregulated, whereas the metabolic pathway-related genes were downregulated in early passages of immortalized hepatocytes compared to the PTHs. Furthermore, expression of hepatocytes function-related genes were repressed in ITH6.1 compared to that of PTHs.

**Conclusion** We believe these cellular expression alterations might cause the resistance of the ITH6.1 cell to HCV infection. This tree shrew liver cell line may be a good resource for the field.

## Key points

- A tree shrew hepatic cell line (ITH6.1) was established.
- ITH6.1 cells could be infected by EV71, but not HCV.
- ITH6.1 had an altered expression profiling compared to the primary hepatocytes.

**Keywords** Immortalized hepatic cell line · Tree shrew · RNA-sequencing · Dynamic expression profile

**Electronic supplementary material** The online version of this article (<https://doi.org/10.1007/s00253-020-10855-x>) contains supplementary material, which is available to authorized users.

✉ Dandan Yu  
yudandan@mail.kiz.ac.cn

✉ Shaozhong Dong  
dsz@imbcams.com.cn

<sup>1</sup> Yunnan Key Laboratory of Vaccine Research and Development on Severe Infectious Diseases, Institute of Medical Biology, Chinese Academy of Medical Sciences & Peking Union Medical College, Kunming 650118, Yunnan, China

<sup>2</sup> Key Laboratory of Animal Models and Human Disease Mechanisms of the Chinese Academy of Sciences and Yunnan Province, and KIZ-CUHK Joint Laboratory of Bioresources and Molecular Research in Common Diseases, Kunming Institute of Zoology, Chinese Academy of Sciences, Kunming 650223, Yunnan, China

<sup>3</sup> Kunming College of Life Science, University of Chinese Academy of Sciences, Kunming 650204, Yunnan, China

<sup>4</sup> National Resource Center for Non-Human Primates, Kunming Primate Research Center, and National Research Facility for Phenotypic & Genetic Analysis of Model Animals (Primate Facility), Kunming Institute of Zoology, Chinese Academy of Sciences, Kunming 650107, Yunnan, China

## Introduction

The Chinese tree shrew is a small squirrel-like mammal. Recent whole-genome sequencing data have shown that tree shrews and primates are more closely related than that of tree shrews and rodents (Fan et al. 2013; Fan et al. 2019; Yao 2017). Given its small body size, easy breeding, rapid reproduction, and low cost, the tree shrew has the potential to become a widely used animal model (Cao et al. 2003; Xiao et al. 2017; Yao 2017). In recent years, tree shrews have already been used as experimental animal models for studying human bacterial and viral infections (Li et al. 2018; Xu et al. 2020a), metabolic disorders (Xiao et al. 2017), eye diseases (Gawne et al. 2017), brain diseases (Fan et al. 2018; Fuchs and Flügge 2002), as well as aging (Fan et al. 2018; Wei et al. 2017) and social behaviors (Ni et al. 2020). Comparison of the skin morphology and structure showed that the Chinese tree shrew had a high similarity to the human, especially for the epidermal appendages (Zhang et al. 2020). There were abundant self-amplifying intermediate progenitor cells in the subventricular zone of the Chinese tree shrew neocortex, which provided direct evidence for a key role of intermediate progenitor cells in brain expansion (Yin et al. 2020).

Since the first report that tree shrew could be infected by hepatitis B virus (HBV) in 1986 (Su et al. 1986), this animal has received much attention for the hepatitis virus infection researches (Li et al. 2018). Analysis of the primary tree shrew hepatocytes (PTHs) and infection of this animal have provided helpful information regarding the pathogenesis of hepatocellular carcinoma caused by viral infections (Guo et al. 2018; Köck et al. 2001; Walter et al. 1996; Yan et al. 1996). Moreover, tree shrew has been used to create animal models for the study of hepatitis C virus (HCV) (Amako et al. 2010; Feng et al. 2017; Xie et al. 1998). Primary tree shrew hepatocytes can be infected with HCV (Barth et al. 2005; Guitart et al. 2005; Yu et al. 2016; Zhao et al. 2002), and the tree shrew mitochondrial antiviral-signaling protein acts as a dual target for HCV innate immune evasion and viral replication (Xu et al. 2020c). However, it is not easy to establish a stable cellular model for PTHs so far, simply because the complexity of primary hepatocyte isolation and purification processes would result in heterogeneity of the harvested primary hepatocytes. It is thus very important to establish a stable and immortalized tree shrew hepatic cell line (Ramboer et al. 2014).

In this study, we used the simian virus 40 large T antigen (SV40LT) (Ahuja et al. 2005; Foddiss et al. 2002) encoded by lentiviral vector to establish an immortalized tree shrew hepatic cell line ITH6.1. We also performed whole transcriptome profiling by using RNA sequencing (RNA-seq) to analyze and classify the differentially expressed genes between the PTHs and different passages of immortalized ITH6.1 cells.

## Materials and methods

### Experimental animals and PTHs isolation

Three male adult tree shrews (~ 1 year old, with a body weight about 130–150 g) were used in this study. One tree shrew was obtained from the Center of Tree Shrew Germplasm Resources, Institute of Medical Biology (IMB), Chinese Academy of Medical Science (CAMS) and Peking Union Medical College, and two tree shrews were introduced from the experimental animal core facility of Kunming Institute of Zoology (KIZ), Chinese Academy of Sciences (CAS). All experiments were approved and performed according to the guidelines approved by the Animal Care and Welfare Committees of the IMB, CAMS (License No. SCXK (Yunnan) K2013–0001), and KIZ, CAS (Approval No: SYDW20110315001). The PTHs were isolated from healthy adult tree shrew as previously described (Salmon et al. 2000; Yu et al. 2016; Zamule et al. 2008).

### Lentiviral transduction

The HEK293T cells were introduced from the Kunming Cell Bank, KIZ, CAS. Cells were seeded into 6-well plates at a density of  $4 \times 10^5$  cells/well. Lentiviral vectors containing 0.4  $\mu\text{g}$  pMD2.G (Addgene, 12259), 0.8  $\mu\text{g}$  psPAX2 (Addgene, 12260), and 1.3  $\mu\text{g}$  M365 plox-Ttag-iresTK-puro (Addgene, 12246) were co-transfected into HEK293T cells using lipofectamine 3000 reagent (Invitrogen, L3000015). The cell culture supernatant was collected after having been filtered with 0.45  $\mu\text{m}$  filters at 48h post-transfection and used for lentiviral infection.

For lentiviral infection, the PTHs were seeded into 6-well plates at a density of  $4 \times 10^5$  cells/well. After 12 h, the culture medium was replaced by the infection mixture (500  $\mu\text{L}$  culture medium with 1  $\mu\text{g}$  polybrene and 500  $\mu\text{L}$  cell culture supernatant that was collected from transfected HEK293T cells). At 48h post-infection, puromycin (1  $\mu\text{g}/\text{mL}$ ) was added to the culture medium, and the puromycin-resistant cells were pooled and expanded. We picked up single-cell colonies from the culture, and finally established the immortalized tree shrew hepatocyte line ITH6.1.

### Growth curve of ITH6.1

The ITH6.1 cells were seeded into 12-well plates with an initial density of  $5.0 \times 10^4$  cells/well. The cells were harvested by trypsinization, and cell number was calculated once a day for five consecutive days using trypan blue exclusion tests, as described in our recent study (Gu et al. 2019). Three wells were included for each count.

## DNA transfection

The ITH6.1 cells were seeded in 24-well plates at a density of  $2 \times 10^4$  cells/well. After 12 h, cells were washed twice with phosphate-buffered saline (PBS), and new culture medium was added. Transfection was performed according to the manufacturer's instructions. In brief, 3  $\mu$ L transfection reagent (Lipofectamine 3000 [Invitrogen, Carlsbad, CA, USA] or Mirus [Mirus Bio, Madison, WI, USA]) and 3  $\mu$ g plasmid DNA were diluted in 50  $\mu$ L Opti-MEM and mixed to form the transfection reagent-plasmid-DNA complex. The mixture was incubated for 15 min at room temperature and then added to cells in a dropwise manner.

## Cell line culture and virus infection

The ITH6.1 cells were seeded in 6-well plates at a density of  $1 \times 10^5$  cells/well for growth for 12 h, and then were infected by enterovirus 71 (EV71, isolated from an HFMD patient whose guardians agreed and signed an informed consent form in Fuyang, China, in 2008, and preserved in CAMS & Peking Union Medical College, Kunming, China) at a multiplicity of infection (MOI) of 1. The cells were harvested at 12-, 24-, 48-, 72-, and 96-h post-infection, respectively.

The Huh7.5.1 cells were introduced from Kunming Cell Bank, KIZ, CAS, and were grown in DMEM (Gibco-BRL, 11965–092) supplemented with 10% (vol/vol) FBS (Gibco-BRL, 10099–141) and  $1 \times$  penicillin/streptomycin (Gibco-BRL, 10378016) at 37 °C in 5% CO<sub>2</sub>. For HCV JFH-1 strain (Japan fulminant hepatitis-1, a kind gift from Dr. Xinwen Chen, Wuhan Institute of Virology, CAS, Wuhan, China) infection, Huh7.5.1 and ITH6.1 cells were infected at different MOI (2, 8, and 32) for 6 h (Yu et al. 2016), respectively, and then were switched to fresh medium after two washes with PBS. The cells were collected at 120 h post-infection. The Huh7.5.1 cells were used as a positive control for robust cellular model of HCV infection in which infectious HCV can be produced and serially passaged to naive cells (Zhong et al. 2005).

## Immunoblotting

Cells were scraped and lysed with RIPA buffer (Thermo Fisher Scientific, Rockford, IL, USA) supplemented with the Halt Protease Inhibitor Cocktail (#78430, Thermo Fisher Scientific, Rockford, IL, USA). Total protein was obtained by centrifugation at 12000g for 10 min, and was quantified with the Pierce™ BCA Protein Assay Kit (Thermo Fisher Scientific Rockford, USA). Proteins (40  $\mu$ g per well) were resolved by SDS-PAGE under reducing conditions and electro-transferred onto a polyvinylidene difluoride

membrane (Immobilon/Millipore, Bedford, MA, USA). Membranes were blocked with 5% BSA in  $1 \times$  Tris-buffered saline (TBS) and incubated with the following antibodies (diluted in  $1 \times$  TBS with 5% BSA or 0.5% nonfat dry milk [w/v]): mouse anti-EV71 VP1 monoclonal antibody (Millipore, Burlington, MA, USA), mouse monoclonal anti-HCV NS3 (Abcam, ab13830), mouse monoclonal anti-HCV core (Thermo Scientific, MA1–080), and horseradish peroxidase-conjugated anti-rabbit IgG antibodies (Cell Signaling Technology, Danvers, MA, USA). Protein bands on the membrane were visualized using the ChemiDoc™ MP imaging system (BioRad, Hercules, CA, USA).

## Library preparation and RNA sequencing

Total RNA was extracted from the PTHs and immortalized cell line at different passages by using TRIzol Reagent (Life; 15596-026) according to the manufacturer's instructions. RNA purity was checked by using the kaiaoK5500 spectrophotometer (Kaiao, Beijing, China). RNA integrity and concentration were assessed by using the RNA Nano 6000 Assay Kit of the Bioanalyzer 2100 system (Agilent Technologies, CA, USA). Only the RNA samples with an A260/A280 ratio between 1.8 and 2.0 and an RNA integrity number > 9 were used for RNA sequencing. For each sample of PTHs or the immortalized cells at different passages, three biological replicates were used for the transcriptomic analysis.

A total of 2  $\mu$ g RNA per sample was used as input material for the RNA sample preparations. Sequencing libraries were generated using the NEBNext® Ultra™ RNA Library Prep Kit for Illumina® (#E7530L; New England Biolabs [NEB], Ipswich, MA, USA) following the manufacturer's recommendations, and index codes were given to each sample. Briefly, mRNA was purified from total RNA using poly-T oligo-attached magnetic beads. Fragmentation was conducted using divalent cations under elevated temperature in NEB Next First Strand Synthesis Reaction Buffer (5 $\times$ ). First-strand cDNA was synthesized using random hexamer primer and RNase H. Second-strand cDNA synthesis was subsequently performed using buffer, dNTPs, DNA polymerase I, and RNase H. The library fragments were purified by using QiaQuick PCR Kits (ID28104; QIAGEN, Germany) and eluted with EB buffer, and then terminal repair, A-tailing, and adapter addition were implemented. The products were retrieved and amplified, and the libraries were completed. The libraries were sequenced on an Illumina platform, and 150 base-pair paired-end reads were generated. The raw data of transcriptomic sequencing have been deposited in genome sequence archive (accession No. CRA002541, <http://gsa.big.ac.cn/gsa/>) (Wang et al. 2017) and the tree shrew database ([www.treeshrewdb.org](http://www.treeshrewdb.org)) (Fan et al. 2019).

## Processing of RNA-seq data

The raw sequencing reads were first processed by Trimmomatic (version 0.36) software to trim the adapter sequence and low-quality sequence using the default parameters (Bolger et al. 2014). After reads filtering, the clean reads were aligned to the high-quality genome of the Chinese tree shrew (Fan et al. 2019) using HISAT2 (version 2.1.0) (Kim et al. 2015). Next, the aligned bam files produced by HISAT2 were used with the featureCounts function of the Subread package (version 1.5.1) (Yang et al. 2013) to assign and count the uniquely mapped fragments to genes using the Chinese tree shrew annotation table file (Fan et al. 2019). Reads counts were normalized to library size by package DESeq2 (version 1.20.2) (Love et al. 2014) in R, and normalized reads were used for calculating the fragments per kilobase of transcript per million fragments mapped (FPKM). These values were transformed to  $\log_2(\text{FPKM} + 1)$  in order to determine the gene expression level. Principle component analysis (PCA) and differential expression analysis were performed using the DESeq2 R package (Love et al. 2014) based on the count table. Genes were identified as differentially expressed between different cell passages if  $|\log_2\text{FoldChange}| > 1$  and  $P_{\text{adj}} < 0.05$ . Gene Ontology (GO) enrichment and Kyoto Encyclopedia of Genes and Genomes (KEGG) enrichment analyses were performed using DAVID (<https://david.ncicrf.gov/>) (Huang et al. 2009); the differentially expressed genes were used as input. We used the Bayesian information criterion super k-means (BICSKmeans) package to determine the number of clusters (Zhang et al. 2013). To balance the tightness and number of clusters, we assigned the parameter “Reg Factor” from 1 to 20, and selected k when the number of clusters was insensitive to the increase of “Reg Factor.” We selected 16 as our “Reg Factor,” and clustered our data into 11 groups by using BICSKmeans. The output from BICSKmeans was imported into “Jave Treeview” (Saldanha 2004) for visualization.

## Statistical analysis

The quantitative values are presented as the mean  $\pm$  standard deviation (SD). All data analyses were performed by using SPSS15.0 (IBM SPSS Inc., Chicago, IL, USA). Student’s *t* test was performed to analyze different significances in the mean values. A *P* value  $< 0.05$  was considered statistically significant.

## Results

### Establishment of the ITH6.1 cell line

The SV40LT (GenBank accession number NP\_043127.1) is frequently used to aid cellular immortalization via multiple mechanisms (Ahuja et al. 2005; Foddiss et al. 2002). We thus

isolated and infected the primary hepatocytes of healthy tree shrews with lentiviral stock solution containing the *SV40LT* gene. After having screened with puromycin and selection of single-cell colonies, we were able to establish the immortalized tree shrew hepatocyte line ITH6.1, which could be continuously subcultured. The immortalized cells exhibited an epithelial-like morphology and showed a similarity to the Huh 7 cells (a human hepatocellular carcinoma derived cell line) (Yoo et al. 1995) (Fig. 1a). Analysis of the growth curve of ITH6.1 showed that this cell line entered a rapid growth period at 48 h post the attachment to the culture dish, and subsequently entered a plateau phase of cell proliferation within 3 days (Fig. 1b). This cell line has been deposited in the China Center for Type Culture Collection (CCTCC No: C201740).

### Transfection of ITH6.1 using DNA transfection reagents

We determined whether ITH6.1 could be transfected by accessible commercial DNA transfection reagents. We transfected the pEGFP-N2 plasmid (Clontech, #6081–1), which expressing enhanced green fluorescent protein (EGFP), into ITH6.1 using two different transfection reagents (Lipofectamine 3000 and Mirus). By fluorescence microscopy, we found that all transfected ITH6.1 expressed a high level of GFP (Fig. 2), suggesting that ITH6.1 could be transfected by DNA transfection reagents.

### ITH6.1 could be infected by EV71, but not HCV

Viral infection in cultured cells triggers a series of immune responses. Thus, cells that are sensitive to viruses are powerful tools for studying the immune response of tree shrew after viral infection (Gu et al. 2019). To determine whether ITH6.1 can be infected by viruses, EV71 and HCV were used to infect the ITH6.1 cells. Though no obvious cytopathic effects were observed in the ITH6.1 cells post-infection, Western blot analysis showed that viral protein 1 (VP1) of EV71 was detected at 12-h post-infection. This result indicated that ITH6.1 can be infected by EV71 (Fig. 3a). However, the VP1 disappeared in the ITH6.1 cells after infection for 72 h or more. We speculated that this was caused by elimination of EV71 proteins due to the incapability of establishing a persistent infection. More focused study will be needed to characterize the mechanism regarding the replication and clearance of EV71 in this cell line.

Hepatocyte receptor for HCV had been reported in tree shrew PTHs (Jia et al. 2008; Tian et al. 2009), and tree shrew PTHs were susceptible to HCV infection (Barth et al. 2005; Guitart et al. 2005; Xu et al. 2020c; Zhao et al. 2002). Challenging ITH6.1 cells at passage 17 (P17) and passage 47

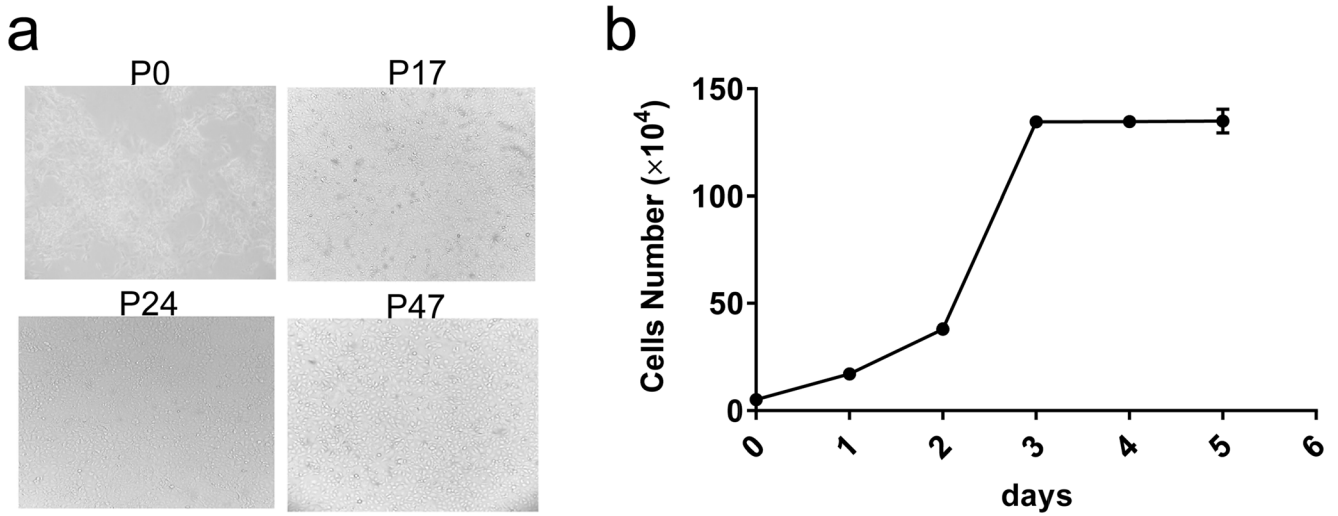


**Fig. 1** Cellular morphology and growth curve of immortalized tree shrew hepatic cell line ITH6.1. **a** Morphology of the ITH6.1 cells at different passages ( $\times 100$  magnification). P0, isolated PTHs from tree shrew liver tissue; P17, cells at passage 17; P24, cells at passage 24; and P47, cells at

passage 47. **b** The ITH6.1 cells have a good proliferation capability. The ITH 6.1 cells were seeded in 24-well plates at a density of  $5 \times 10^4$  cells/well. Cells were harvested by trypsinization and counted once per day. Three wells were included for each cell count. Bar, mean  $\pm$  SD

(P47) with HCV showed no successful infection, as we found no production of HCV core and NS3 proteins after HCV infection for 5 days. Increase of the HCV MOI from 2 to 32 still did not result in a successful infection (Fig. 4b). Conversely, the expression levels of HCV CORE and NS3 proteins were elevated in Huh7.5.1, a robust cell culture model of HCV infection (Zhong et al. 2005), along with the increased MOI

(Fig. 3b). These results suggested ITH6.1 could be used for testing other viral infections, but not be suitable for HCV infection and replication. Note that a more sensitive detection method, such as quantitative real-time PCR detection of HCV genome, should be performed to offer confirmatory information regarding the susceptibility of PTHs and ITH6.1 cells to HCV.

**Fig. 2** Transfection of ITH6.1 using different transfection reagents. The ITH6.1 cells were transfected with the pEGFP-N2 by using Lipofectamine 3000 (Lipo3000) or Mirus transfection reagent. The expression of GFP was observed by fluorescence microscopy at 24 h after the transfection ( $\times 100$  magnification)

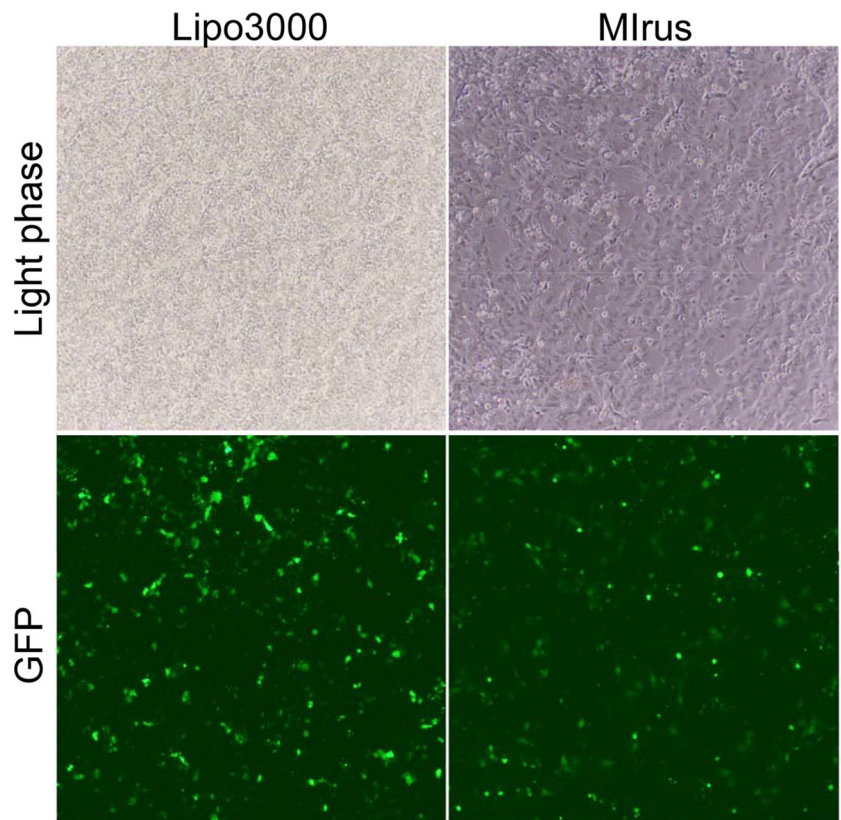
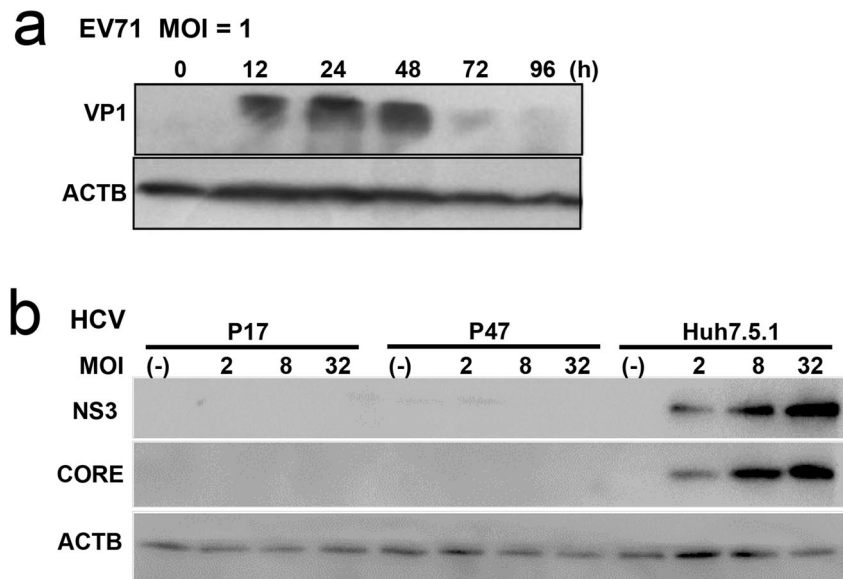


**Fig. 3** The ITH6.1 cells can be infected by EV71, but not HCV. **a** Successful infection of ITH6.1 by EV71. Cells were infected with or without EV71 (MOI = 1) and were harvested at the indicated times post infection. Cell lysates were immunoblotted using anti-EV71 VP1 antibody. **b** HCV infection of the ITH6.1 cells at different passages (P17 and P47) and the Huh7.5.1 cells. Cells were infected with or without (–) different titers of HCV for 5 days before the harvest. Cell lysates were immunoblotted using the anti-HCV core antibody and anti-HCV NS3 antibody, respectively. The ACTB ( $\beta$ -actin) was used as the loading control



### Transcriptomic profiling revealed by RNA-Seq

To understand why the PTHs lost the capability to sustain the HCV infection and replication during the transformation, we analyzed the gene expression changes between the PTHs and the immortalized cells at different passages. Two PTH samples (PTH-I and PTH-II) and different passages of the ITH6.1 cells (passage 9, ITH6.1-P9; passage 17, ITH6.1-P17; passage 24, ITH6.1-P24; passage 33, ITH6.1-P33; passage 47, ITH6.1-P47) were selected for total RNA extraction and transcriptome analysis. We used the principal component (PC) analysis to show the overall clustering pattern of the samples. The PTHs, early

passage of immortalized cells (early passage cells: ITH6.1-P9, ITH6.1-P17 and ITH6.1-P24), and long passage immortalized cells (immortalized cells: ITH6.1-P33 and ITH6.1-P47) were clearly separated from each other in the PC map (Fig. 4a). We further determined the differentially expressed genes (DEGs) among the three main groups of cells. Between the PTHs and early passage cells, a total of 3618 genes were downregulated and 2532 genes were upregulated. When the early passage cells were compared with the immortalized cells, a total of 1995 genes were downregulated and 1615 genes were upregulated. The top 20 genes showing the most significant expression changes between the PTHs and early passage cells (Table S1) were not

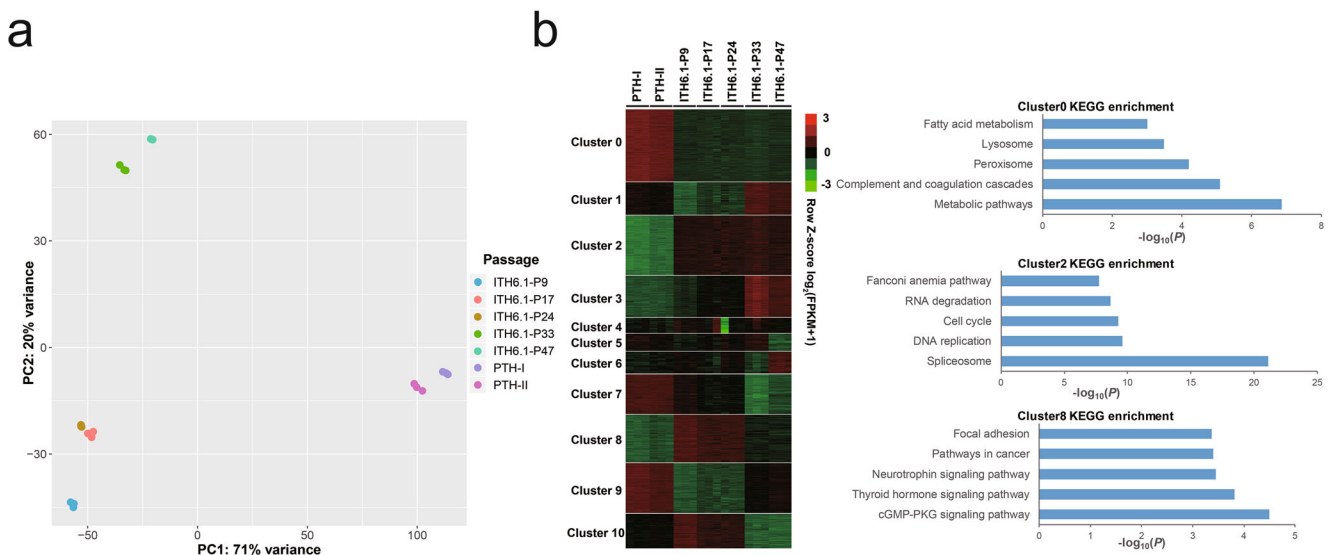


**Fig. 4** RNA-seq analysis of the tree shrew hepatocytes (PTHs) and different passages of the ITH6.1 cells. **a** Principal component analysis of PTHs from two tree shrews (PTH-I and PTH-II) and different passages of the ITH6.1 cells. Each sample has three biological replicates. **b** Heat map of gene expression pattern in the PTHs and different passages of the

ITH6.1 cells and pathway enrichments. Differentially expressed genes (DEGs) between different samples were defined if  $|\log_2\text{FoldChange}| > 1$  and  $P_{\text{adj}} < 0.05$ . GO and KEGG enrichment analyses were analyzed using DAVID (<https://david.ncifcrf.gov/>), with the DEGs as the input

overlapped with those between the early passage cells and the immortalized cells (Table S2).

We constructed the clusters based on gene expression patterns among these samples. A total of 11 clusters could be observed for cells during the transformation (Fig. 4b). We found that genes in Cluster 2 were upregulated in the ITH6.1 cells at different passages compared with PTHs, and mainly contained genes involved in DNA replication, RNA degradation, and cell cycle (Fig. 4b). This pattern was consistent with the characteristics of the primary hepatocyte immortalization (Ramboer et al. 2014). In addition, the genes in Cluster 0 were downregulated in ITH6.1 compared with PTHs, and genes in this cluster were involved in cellular metabolic pathways and fatty acid metabolism (Fig. 4b). Cluster 8 was composed of genes involved in the neurotrophin signal transduction pathway, thyroid signaling, and cGMP-PKG signaling, and genes in this cluster were increased in early passage cells relative to those of the PTHs, and then decreased in the immortalized cells (Fig. 4b).

### Changes of liver cell markers and related genes

The process of HCV entry into target cells represented the first step in the viral life cycle (Moradpour et al. 2007). We first assessed the mRNA levels of the known HCV entry factors, including CD81, SR-BI, CLDN1, and OCLN, in PTHs and ITH6.1 of different passages. Compared with PTHs, there were differences of the mRNA levels for the four HCV entry factors in cells at different passages, and the four HCV entry factors were all expressed in ITH6.1 (Fig. 5a). Moreover, the four HCV entry factors of the Chinese tree shrew had a considerably high protein sequence identity with those of human (CD81, 96%; SR-BI, 87%; CLDN1, 93%; OCLN, 88%) according to the previous study (Tong et al. 2011) and the updated genome information (Fan et al. 2019). Based on these results and the above HCV infection assay (Fig. 3b), we speculated that the ITH6.1 cells might not have a problem for HCV entry process, but did not support HCV replication. A direct transfection of the HCV RNA genome into the ITH6.1 cells would help to confirm this speculation.

We analyzed the mRNA levels of hepatocyte marker genes in PTHs and ITH6.1 cells. The mRNA level of  $\beta$ -actin was stable (Fig. 5b), whereas that of the albumin (ALB) (Wang et al. 2003) was downregulated in the ITH6.1 cells at different passages. There was no remarkable change of the mRNA levels of *cytokeratin18* (CK18) (Zatloukal et al. 2000) and *apolipoprotein E* (ApoE) (Hamilton et al. 1990) at different time points of immortalization (Fig. 5b). The PTHs have played a major role in drug metabolism, which is closely related to cytochrome P450 (CYP450) enzyme family (van der Weide and Steijns 1999). We found that the mRNA levels of the CYP450 family key members, *CYP2E1* and *CYP1A2*, were reduced in later passage of the ITH6.1 cells, whereas

the mRNA levels of *CYP2U1* and *CYP3A4* did not show a dramatic decreasing pattern as those of *CYP2E1* and *CYP1A2* (Fig. 5c) (van der Weide and Steijns 1999).

We further analyzed the mRNA levels of hepatocyte nuclear factors (HNF), which are a group of transcriptional factors mainly expressed in hepatocytes and are essential for the development, maturation, and differentiation of hepatocytes, glycogen transport, and metabolism (Cheng et al. 2019; Wiwi and Waxman 2004). The mRNA levels of the HNF family members did not show a consistent pattern (Fig. 5d). Analyses for mRNA levels of several innate immune receptors, such as TLRs (Yu et al. 2016), STING (Xu et al. 2020b) and MDA5 (Xu et al. 2016), showed that these genes were decreased in different passages of ITH6.1 compared with the PTHs (Fig. 5e).

Taken together, our analysis of the related genes that are involved in liver function and innate immune response did identify several genes showing a passage-dependent change during the immortalization, but others did not provide any useful information to characterize the cellular alterations that account for the resistance of HCV infection in the immortalized cell lines.

### Discussion

Tree shrew is an experimental animal which has been extensively used in biomedical researches (Li et al. 2018; Xiao et al. 2017; Yao 2017). Many recent studies have reported the immune responses and pathological and physiological changes of the tree shrew after viral infections (Li et al. 2018; Xiao et al. 2017; Xu et al. 2020a; Xu et al. 2019; Yao 2017; Zhang et al. 2019). We performed a genome sequencing of the Chinese tree shrew (Fan et al. 2019; Fan et al. 2014) and characterized the genetic features of the innate immunity-related genes of this species (Xu et al. 2016; Xu et al. 2020b; Xu et al. 2020c; Yao 2017; Yu et al. 2016). Although lots of efforts have been made to create animal models using tree shrews, there are only few tree shrew immortalized cell lines available (Gu et al. 2019; Yin et al. 2019), and none could meet the needs for studying HBV and HCV in vitro. In this study, we aimed to establish a tree shrew immortalized hepatocyte cell line by introducing the SV40LT (Ahuja et al. 2005; Foddiss et al. 2002) into tree shrew PTHs via lentiviral infection. We were able to get an immortalized liver cell line, which showed a reasonably good proliferation capacity and could be transfected by using commercial transfection reagents. However, this cell line could not be infected by HCV, although it could be infected by EV71 and other viruses (author's unpublished data). Therefore, this cell line might be a resource for characterize viral response of other viruses instead of HCV.

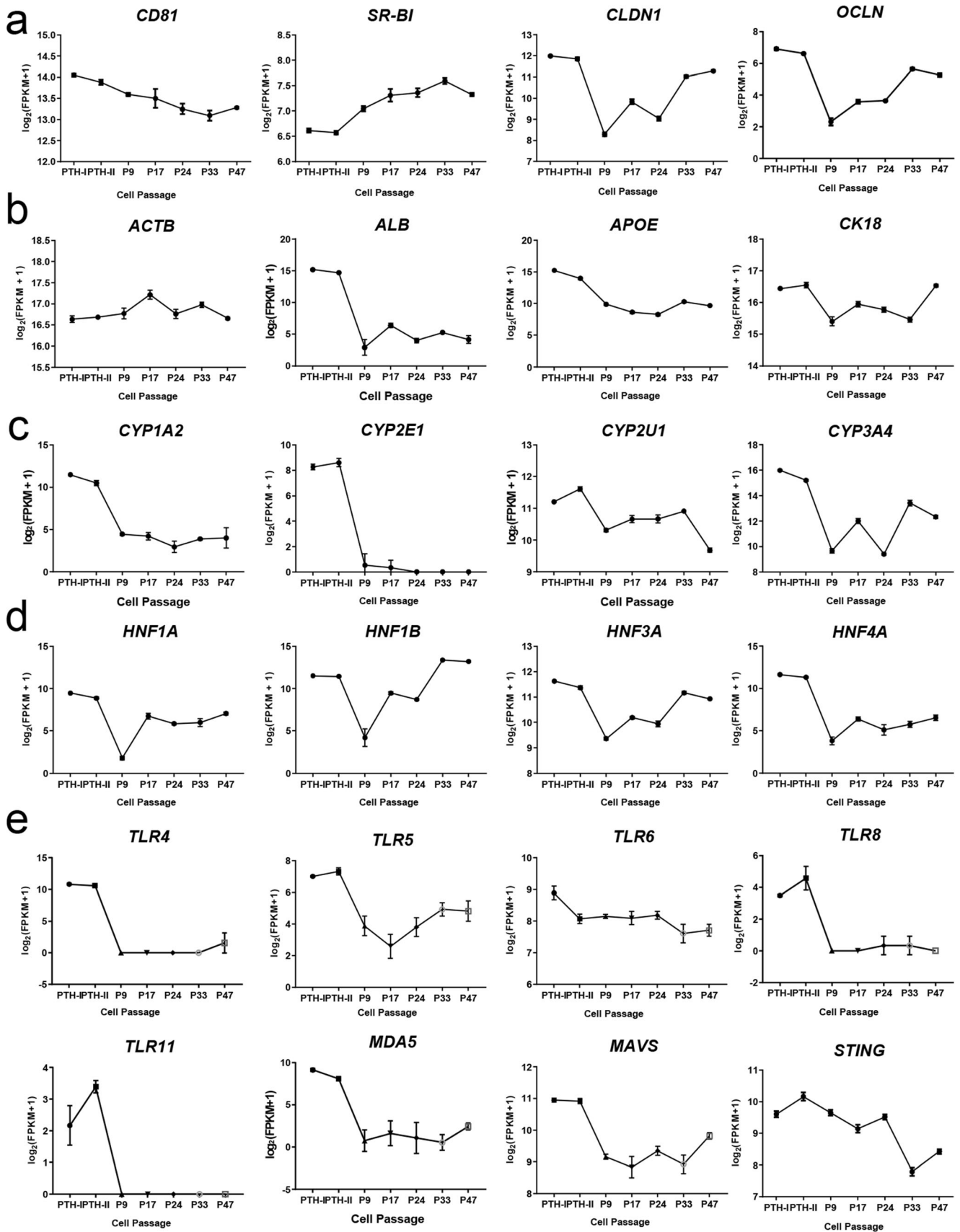


**Fig. 5** Transcriptional changes of liver function-related genes during the immortalization of the tree shrew liver cells. The mRNA levels of the major HCV entry receptors **a**, molecular markers of hepatocytes **b**, CYP450 enzyme **c**, HNFs **d**, and innate immune genes **e** in tree shrew PTHs and immortalized liver cells at different passages. The  $\beta$ -actin gene was used as the reference gene

To explore the underlying reason why HCV could not infect the immortalized ITH6.1 cells, we performed the RNA-sequencing to learn the overall change of gene expression between the PTHs and different passages of ITH6.1. We could clearly discern different clusters of genes that had a dramatic change during the transformation and immortalization. In particular, genes related to RNA degradation, cell cycle, DNA replication, and cleavage were among the list of top genes, and the change of these genes might enhance the proliferation abilities after immortalization (Maqsood et al. 2013; Ramboer et al. 2014). The major HCV entry receptors were all expressed in different passages of ITH6.1 (Fig. 5a), which indicated that the entry of HCV to this cell line might not be hampered. We also found that genes related to multiple signaling pathways, such as neural signaling, thyroxine signaling, cGMP-protein kinase G signaling, and immune responses, were altered during the immortalization, which might be compatible with the change of cellular phenotypes of the ITH6.1 cells. Of note, the mRNA levels of albumin (ALB) and some members of CYP450 and HNF families were also changed during the immortalization (Fig. 5c and d), which might account for the reason why ITH6.1 was resistant to HCV infection (Cheng et al. 2019; Hamilton et al. 1990; van der Weide and Steijns 1999). However, it would be hard to draw a clear picture regarding the trajectory of the liver cell immortalization in this study.

In summary, we established an immortalized cell line from the Chinese tree shrew primary hepatocytes, which maintained a high proliferation rate. This cell line could be transfected by commercial transfection reagents and infected by EV71, but not HCV. Analysis of the entire transcriptomic profiling of PTHs and ITH6.1 cells at different passages during the immortalization identified a variety of DEGs among the PTHs, early passage cells (ITH6.1-P9, ITH6.1-P17, and ITH6.1-P24) and immortalized cells (ITH6.1-P33 and ITH6.1-P47), which constitute the genetic basis for recognition of the cell source and alteration of cellular phenotypes. We believe that this cell line may be of some usage for studying the cell signaling in response to viral infections and drug treatment.

**Acknowledgements** We thank the two anonymous reviewers for their helpful comments on the early version of this paper.

**Authors' contribution** YGY, SD, and DY conceived and designed the research. NM, DY, XZ, and TG conducted the experiments. YW, NM, and TG analyzed the data. XZ, DY, TG, and YGY wrote the manuscript. All authors read and approved the manuscript.

**Funding** This study was supported by Yunnan Province (2018ZF006 and 2018FB046), the Chinese Academy of Sciences (CAS “Light of West China” Program xzbzg-zdsys-201909), and National Natural Science Foundation of China (81571998 and U1902215).

## Compliance with ethical standards

**Conflict of interest** The authors declare that they have no conflict of interest.

**Ethical approval** All experiments were approved and performed according to the guidelines approved by the Animal Care and Welfare Committee of the Institute of Medical Biology, Chinese Academy of Medical Sciences.

## References

- Ahuja D, Sáenz-Robles MT, Pipas JM (2005) SV40 large T antigen targets multiple cellular pathways to elicit cellular transformation. *Oncogene* 24(52):7729–7745. <https://doi.org/10.1038/sj.onc.1209046>
- Amako Y, Tsukiyama-Kohara K, Katsume A, Hirata Y, Sekiguchi S, Tobita Y, Hayashi Y, Hishima T, Funata N, Yonekawa H, Kohara M (2010) Pathogenesis of hepatitis C virus infection in *Tupaia belangeri*. *J Virol* 84(1):303–311. <https://doi.org/10.1128/JVI.01448-09>
- Barth H, Cerino R, Arcuri M, Hoffmann M, Schurmann P, Adah MI, Gissler B, Zhao X, Ghisetti V, Lavezzo B, Blum HE, von Weizsacker F, Vitelli A, Scarselli E, Baumert TF (2005) Scavenger receptor class B type I and hepatitis C virus infection of primary *tupaia* hepatocytes. *J Virol* 79(9):5774–5785. <https://doi.org/10.1128/JVI.79.9.5774-5785.2005>
- Bolger AM, Lohse M, Usadel B (2014) Trimmomatic: a flexible trimmer for Illumina sequence data. *Bioinformatics* 30(15):2114–2120. <https://doi.org/10.1093/bioinformatics/btu170>
- Cao J, Yang E-B, Su J-J, Li Y, Chow P (2003) The tree shrews: adjuncts and alternatives to primates as models for biomedical research. *J Med Primatol* 32(3):123–130. <https://doi.org/10.1034/j.1600-0684.2003.00022.x>
- Cheng Z, He Z, Cai Y, Zhang C, Fu G, Li H, Sun W, Liu C, Cui X, Ning B, Xiang D, Zhou T, Li X, Xie W, Wang H, Ding J (2019) Conversion of hepatoma cells to hepatocyte-like cells by defined hepatocyte nuclear factors. *Cell Res* 29(2):124–135. <https://doi.org/10.1038/s41422-018-0111-x>
- Fan Y, Huang Z-Y, Cao C-C, Chen C-S, Chen Y-X, Fan D-D, He J, Hou H-L, Hu L, Hu X-T, Jiang X-T, Lai R, Lang Y-S, Liang B, Liao S-G, Mu D, Ma Y-Y, Niu Y-Y, Sun X-Q, Xia J-Q, Xiao J, Xiong Z-Q, Xu L, Yang L, Zhang Y, Zhao W, Zhao X-D, Zheng Y-T, Zhou J-M, Zhu Y-B, Zhang G-J, Wang J, Yao Y-G (2013) Genome of the Chinese tree shrew. *Nat Commun* 4:1426. <https://doi.org/10.1038/ncomms2416>
- Fan Y, Yu D, Yao Y-G (2014) Tree shrew database (TreeshrewDB): a genomic knowledge base for the Chinese tree shrew. *Sci Rep* 4: 7145. <https://doi.org/10.1038/srep07145>
- Fan Y, Luo R, Su LY, Xiang Q, Yu D, Xu L, Chen J-Q, Bi R, Wu D-D, Zheng P, Yao Y-G (2018) Does the genetic feature of the Chinese tree shrew (*Tupaia belangeri chinensis*) support its potential as a viable model for Alzheimer's disease research? *J Alzheimers Dis* 61(3):1015–1028. <https://doi.org/10.3233/JAD-170594>
- Fan Y, Ye M-S, Zhang J-Y, Xu L, Yu D, Gu T, Yao Y-L, Chen J-Q, Lv L-B, Zheng P, Wu D-D, Zhang G-J, Yao Y-G (2019) Chromosomal level assembly and population sequencing of the Chinese tree shrew

- genome. *Zool Res* 40(6):506–521. <https://doi.org/10.24272/j.issn.2095-8137.2019.063>
- Feng Y, Feng Y-M, Lu C, Han Y, Liu L, Sun X, Dai J, Xia X (2017) Tree shrew, a potential animal model for hepatitis C, supports the infection and replication of HCV *in vitro* and *in vivo*. *J Gen Virol* 98(8):2069–2078. <https://doi.org/10.1099/jgv.0.000869>
- Foddiss R, De Rienzo A, Broccoli D, Bocchetta M, Stekala E, Rizzo P, Tosolini A, Grobelny JV, Jhanwar SC, Pass HI, Testa JR, Carbone M (2002) SV40 infection induces telomerase activity in human mesothelial cells. *Oncogene* 21(9):1434–1442. <https://doi.org/10.1038/sj.onc.1205203>
- Fuchs E, Flügge G (2002) Social stress in tree shrews: effects on physiology, brain function, and behavior of subordinate individuals. *Pharmacol Biochem Behav* 73(1):247–258. [https://doi.org/10.1016/s0091-3057\(02\)00795-5](https://doi.org/10.1016/s0091-3057(02)00795-5)
- Gawne TJ, Ward AH, Norton TT (2017) Long-wavelength (red) light produces hyperopia in juvenile and adolescent tree shrews. *Vis Res* 140:55–65. <https://doi.org/10.1016/j.visres.2017.07.011>
- Gu T, Yu D, Li Y, Xu L, Yao Y-L, Yao Y-G (2019) Establishment and characterization of an immortalized renal cell line of the Chinese tree shrew (*Tupaia belangeri chinensis*). *Appl Microbiol Biotechnol* 103(5):2171–2180. <https://doi.org/10.1007/s00253-019-09615-3>
- Guitart A, Riezu-Boj J-I, Elizalde E, Larrea E, Berasain C, Aldabe R, Civeira MP, Prieto J (2005) Hepatitis C virus infection of primary tupaia hepatocytes leads to selection of quasispecies variants, induction of interferon-stimulated genes and NF- $\kappa$ B nuclear translocation. *J Gen Virol* 86(Pt 11):3065–3074. <https://doi.org/10.1099/vir.0.81273-0>
- Guo W-N, Zhu B, Ai L, Yang D-L, Wang B-J (2018) Animal models for the study of hepatitis B virus infection. *Zool Res* 39(1):25–31. <https://doi.org/10.24272/j.issn.2095-8137.2018.013>
- Hamilton RL, Wong JS, Guo LS, Krisans S, Havel RJ (1990) Apolipoprotein E localization in rat hepatocytes by immunogold labeling of cryothin sections. *J Lipid Res* 31(9):1589–1603
- Huang DW, Sherman BT, Lempicki RA (2009) Systematic and integrative analysis of large gene lists using DAVID bioinformatics resources. *Nat Protoc* 4(1):44–57. <https://doi.org/10.1038/nprot.2008.211>
- Jia ZS, Du DW, Lei YF, Wei X, Yin W, Ma L, Lian JQ, Wang PZ, Li D, Zhou YX (2008) Scavenger receptor class B type I mediates cell entry of hepatitis C virus. *J Int Med Res* 36(6):1319–1325. <https://doi.org/10.1177/147323000803600620>
- Kim D, Langmead B, Salzberg SL (2015) HISAT: a fast spliced aligner with low memory requirements. *Nat Methods* 12(4):357–360. <https://doi.org/10.1038/nmeth.3317>
- Köck J, Nassal M, MacNelly S, Baumert TF, Blum HE, von Weizsäcker F (2001) Efficient infection of primary tupaia hepatocytes with purified human and woolly monkey hepatitis B virus. *J Virol* 75(11):5084–5089. <https://doi.org/10.1128/JVI.75.11.5084-5089.2001>
- Li R, Zanin M, Xia X, Yang Z (2018) The tree shrew as a model for infectious diseases research. *J Thorac Dis* 10(Suppl 19):S2272–S2279. <https://doi.org/10.21037/jtd.2017.12.121>
- Love MI, Huber W, Anders S (2014) Moderated estimation of fold change and dispersion for RNA-seq data with DESeq2. *Genome Biol* 15(12):550. <https://doi.org/10.1186/s13059-014-0550-8>
- Maqsood MI, Matin MM, Bahrami AR, Ghasroldasht MM (2013) Immortality of cell lines: challenges and advantages of establishment. *Cell Biol Int* 37(10):1038–1045. <https://doi.org/10.1002/cbin.10137>
- Moradpour D, Penin F, Rice CM (2007) Replication of hepatitis C virus. *Nat Rev Microbiol* 5(6):453–463. <https://doi.org/10.1038/nrmicro1645>
- Ni R-J, Tian Y, Dai X-Y, Zhao L-S, Wei J-X, Zhou J-N, Ma X-H, Li T (2020) Social avoidance behavior in male tree shrews and prosocial behavior in male mice toward unfamiliar conspecifics in the laboratory. *Zool Res* 41(3):258–272. <https://doi.org/10.24272/j.issn.2095-8137.2020.034>
- Ramboer E, De Craene B, De Kock J, Vanhaecke T, Berx G, Rogiers V, Vinken M (2014) Strategies for immortalization of primary hepatocytes. *J Hepatol* 61(4):925–943. <https://doi.org/10.1016/j.jhep.2014.05.046>
- Saldanha AJ (2004) Java Treeview—extensible visualization of microarray data. *Bioinformatics* 17:17–3248. <https://doi.org/10.1093/bioinformatics/bth349>
- Salmon P, Oberholzer J, Occhiodoro T, Morel P, Lou JN, Trono D (2000) Reversible immortalization of human primary cells by lentivector-mediated transfer of specific genes. *Mol Ther* 2(4):404–414. <https://doi.org/10.1006/mthe.2000.0141>
- Su J, Yan R, Gan Y, Zhou D, Huang D, Huang G (1986) A study of experimental infection by human hepatitis B virus (HBV) in adult tree shrew. *Shanghai Lab Anim Sci* 6(4):193–198
- Tian Z-F, Shen H, Fu X-H, Chen Y-C, Blum HE, Baumert TF, Zhao X-P (2009) Interaction of hepatitis C virus envelope glycoprotein E2 with the large extracellular loop of tupaia CD81. *World J Gastroenterol* 15(2):240–244. <https://doi.org/10.3748/wjg.15.240>
- Tong Y, Zhu Y, Xia X, Liu Y, Feng Y, Hua X, Chen Z, Ding H, Gao L, Wang Y, Feitelson MA, Zhao P, Qi Z-T (2011) Tupaia CD81, SR-BI, claudin-1, and occludin support hepatitis C virus infection. *J Virol* 85(6):2793–2802. <https://doi.org/10.1128/jvi.01818-10>
- van der Weide J, Steijns LS (1999) Cytochrome P450 enzyme system: genetic polymorphisms and impact on clinical pharmacology. *Ann Clin Biochem* 36(Pt 6):722–729. <https://doi.org/10.1177/000456329903600604>
- Walter E, Keist R, Niederöst B, Pult I, Blum HE (1996) Hepatitis B virus infection of tupaia hepatocytes *in vitro* and *in vivo*. *Hepatology* 24(1):1–5. <https://doi.org/10.1002/hep.510240101>
- Wang X, Ge S, McNamara G, Hao Q-L, Crooks GM, Nolta JA (2003) Albumin-expressing hepatocyte-like cells develop in the livers of immune-deficient mice that received transplants of highly purified human hematopoietic stem cells. *Blood* 101(10):4201–4208. <https://doi.org/10.1182/blood-2002-05-1338>
- Wang Y, Song F, Zhu J, Zhang S, Yang Y, Chen T, Tang B, Dong L, Ding N, Zhang Q, Bai Z, Dong X, Chen H, Sun M, Zhai S, Sun Y, Yu L, Lan L, Xiao J, Fang X, Lei H, Zhang Z, Zhao W (2017) GSA: genome sequence archive\*. *Genomics Proteomics Bioinforma* 15(1):14–18. <https://doi.org/10.1016/j.gpb.2017.01.001>
- Wei S, Hua H-R, Chen Q-Q, Zhang Y, Chen F, Li S-Q, Li F, Li J-L (2017) Dynamic changes in DNA methylation in the tree shrew (*Tupaia belangeri chinensis*) brain during postnatal development and aging. *Zool Res* 38(2):96–102. <https://doi.org/10.24272/j.issn.2095-8137.2017.013>
- Wiwi CA, Waxman DJ (2004) Role of hepatocyte nuclear factors in growth hormone-regulated, sexually dimorphic expression of liver cytochromes P450. *Growth Factors* 22(2):79–88. <https://doi.org/10.1080/08977190410001715172>
- Xiao J, Liu R, Chen C-S (2017) Tree shrew (*Tupaia belangeri*) as a novel laboratory disease animal model. *Zool Res* 38(3):127–137. <https://doi.org/10.24272/j.issn.2095-8137.2017.033>
- Xie ZC, Riezu-Boj JI, Lasarte JJ, Guillen J, Su JH, Civeira MP, Prieto J (1998) Transmission of hepatitis C virus infection to tree shrews. *Virology* 244(2):513–520. <https://doi.org/10.1006/viro.1998.9127>
- Xu L, Yu D, Fan Y, Peng L, Wu Y, Yao Y-G (2016) Loss of RIG-I leads to a functional replacement with MDA5 in the Chinese tree shrew. *Proc Natl Acad Sci U S A* 113(39):10950–10955. <https://doi.org/10.1073/pnas.1604939113>
- Xu S, Li X, Yang J, Wang Z, Jia Y, Han L, Wang L, Zhu Q (2019) Comparative pathogenicity and transmissibility of pandemic H1N1, avian H5N1, and human H7N9 influenza viruses in tree shrews. *Front Microbiol* 10:2955. <https://doi.org/10.3389/fmicb.2019.02955>

- Xu L, Yu D-D, Ma Y-H, Yao Y-L, Luo R-H, Feng X-L, Cai H-R, Han J-B, Wang X-H, Li M-H, Ke C-W, Zheng Y-T, Yao Y-G (2020a) COVID-19-like symptoms observed in Chinese tree shrews infected with SARS-CoV-2. *Zool Res*:1–5. <https://doi.org/10.24272/j.issn.2095-8137.2020.053>
- Xu L, Yu D, Peng L, Wu Y, Fan Y, Gu T, Yao Y-L, Zhong J, Chen X, Yao Y-G (2020b) An alternative splicing of *Tupaia* STING modulated anti-RNA virus responses by targeting MDA5-LGP2 and IRF3. *J Immunol* 204(12):3191–3204. <https://doi.org/10.4049/jimmunol.1901320>
- Xu L, Yu D, Yao Y-L, Gu T, Zheng X, Wu Y, Luo R-H, Zheng Y-T, Zhong J, Yao Y-G (2020c) *Tupaia* MAVS is a dual target during HCV infection for innate immune evasion and viral replication via NF- $\kappa$ B. *J Immunol* <https://doi.org/10.4049/jimmunol.2000376>
- Yan RQ, Su JJ, Huang DR, Gan YC, Yang C, Huang GH (1996) Human hepatitis B virus and hepatocellular carcinoma. I Experimental infection of tree shrews with hepatitis B virus. *J Cancer Res Clin Oncol* 122(5):283–288. <https://doi.org/10.1007/bf01261404>
- Yang L, Smyth GK, Wei S (2013) featureCounts: an efficient general purpose program for assigning sequence reads to genomic features. *Bioinformatics* 7(7):7. <https://doi.org/10.1093/bioinformatics/btt656>
- Yao Y-G (2017) Creating animal models, why not use the Chinese tree shrew (*Tupaia belangeri chinensis*)? *Zool Res* 38(3):118–126. <https://doi.org/10.24272/j.issn.2095-8137.2017.032>
- Yin B, Song Q, Chen L, Li X, Han Y, Wang X, Dai J, Sun X (2019) Establishment of an immortalized intestinal epithelial cell line from tree shrews by lentivirus-mediated hTERT gene transduction. *Cytotechnology* 71(1):107–116. <https://doi.org/10.1007/s10616-018-0270-0>
- Yin C, Zhou X, Yao Y-G, Wang W, Wu Q, Wang X (2020) Abundant self-amplifying intermediate progenitors in the subventricular zone of the Chinese tree shrew neocortex. *Cereb Cortex* 30(5):3370–3380. <https://doi.org/10.1093/cercor/bhz315>
- Yoo BJ, Selby MJ, Choe J, Suh BS, Choi SH, Joh JS, Nuovo GJ, Lee HS, Houghton M, Han JH (1995) Transfection of a differentiated human hepatoma cell line (Huh7) with in vitro-transcribed hepatitis C virus (HCV) RNA and establishment of a long-term culture persistently infected with HCV. *J Virol* 69(1):32–38. <https://doi.org/10.1128/JVI.69.1.32-38.1995>
- Yu D, Wu Y, Xu L, Fan Y, Peng L, Xu M, Yao Y-G (2016) Identification and characterization of toll-like receptors (TLRs) in the Chinese tree shrew (*Tupaia belangeri chinensis*). *Dev Comp Immunol* 60:127–138. <https://doi.org/10.1016/j.dci.2016.02.025>
- Zamule SM, Strom SC, Omiecinski CJ (2008) Preservation of hepatic phenotype in lentiviral-transduced primary human hepatocytes. *Chem Biol Interact* 173(3):179–186. <https://doi.org/10.1016/j.cbi.2008.03.015>
- Zatloukal K, Stumptner C, Lehner M, Denk H, Baribault H, Eshkind LG, Franke WW (2000) Cytokeratin 8 protects from hepatotoxicity, and its ratio to cytokeratin 18 determines the ability of hepatocytes to form Mallory bodies. *Am J Pathol* 156(4):1263–1274. [https://doi.org/10.1016/S0002-9440\(10\)64997-8](https://doi.org/10.1016/S0002-9440(10)64997-8)
- Zhang W, Liu Y, Sun N, Wang D, Boyd-Kirkup J, Dou X, Han JD (2013) Integrating genomic, epigenomic, and transcriptomic features reveals modular signatures underlying poor prognosis in ovarian cancer. *Cell Rep* 4(3):542–553. <https://doi.org/10.1016/j.celrep.2013.07.010>
- Zhang N-N, Zhang L, Deng Y-Q, Feng Y, Ma F, Wang Q, Ye Q, Han Y, Sun X, Zhang F-C, Qi X, Wang G, Dai J, Xia X, Qin C-F (2019) Zika virus infection in *Tupaia belangeri* causes dermatological manifestations and confers protection against secondary infection. *J Virol* 93(8):e01982–e01918. <https://doi.org/10.1128/JVI.01982-18>
- Zhang J, Luo R-C, Man X-Y, Lv L-B, Yao Y-G, Zheng M (2020) The anatomy of the skin of the Chinese tree shrew is very similar to that of human skin. *Zool Res* 41(2):208–212. <https://doi.org/10.24272/j.issn.2095-8137.2020.028>
- Zhao X, Tang Z-Y, Klumpp B, Wolff-Vorbeck G, Barth H, Levy S, von Weizsäcker F, Blum HE, Baumert TF (2002) Primary hepatocytes of *Tupaia belangeri* as a potential model for hepatitis C virus infection. *J Clin Invest* 109(2):221–232. <https://doi.org/10.1172/JCI13011>
- Zhong J, Gastaminza P, Cheng G, Kapadia S, Kato T, Burton DR, Wieland SF, Uprichard SL, Wakita T, Chisari FV (2005) Robust hepatitis C virus infection in vitro. *Proc Natl Acad Sci U S A* 102(26):9294–9299. <https://doi.org/10.1073/pnas.0503596102>

**Publisher's note** Springer Nature remains neutral with regard to jurisdictional claims in published maps and institutional affiliations.

## Applied Microbiology and Biotechnology

### Establishment and transcriptomic features of an immortalized hepatic cell line of the Chinese tree shrew

Xuemei Zhang<sup>1</sup>, Dandan Yu<sup>2,\*</sup>, Yong Wu<sup>2</sup>, Tianle Gu<sup>2,3</sup>, Na Ma<sup>1</sup>, Shaozhong Dong<sup>1,\*</sup>, Yong-Gang Yao<sup>2,3,4</sup>

<sup>1</sup> Yunnan Key Laboratory of Vaccine Research and Development on Severe Infectious Diseases, Institute of Medical Biology, Chinese Academy of Medical Sciences & Peking Union Medical College, Kunming, Yunnan 650118, China

<sup>2</sup> Key Laboratory of Animal Models and Human Disease Mechanisms of the Chinese Academy of Sciences and Yunnan Province, and KIZ-CUHK Joint Laboratory of Bioresources and Molecular Research in Common Diseases, Kunming Institute of Zoology, Chinese Academy of Sciences, Kunming, Yunnan 650223, China

<sup>3</sup> Kunming College of Life Science, University of Chinese Academy of Sciences, Kunming, Yunnan 650204, China

<sup>4</sup> National Resource Center for Non-Human Primates, Kunming Primate Research Center, and National Research Facility for Phenotypic & Genetic Analysis of Model Animals (Primate Facility), Kunming Institute of Zoology, Chinese Academy of Sciences, Kunming, Yunnan 650107, China

\*Corresponding Author: Prof. Shaozhong Dong, [dsz@imbcams.com.cn](mailto:dsz@imbcams.com.cn), or Dandan Yu, [yudandan@mail.kiz.ac.cn](mailto:yudandan@mail.kiz.ac.cn)

Table S1: The top 20 genes with altered expression between the PTHs (PTH-I and PTH-II) and early passages cells (ITH6.1-P9, ITH6.1-P17 and ITH6.1-P24)

Gene name	Log <sub>2</sub> fold change	Description	Functional annotation	<i>P</i> <sub>adj</sub>
Upregulated genes				
<i>DLK1</i>	12.03	delta-like 1 homolog	calcium ion binding	1.64E-35
<i>GJD2</i>	11.14	gap junction protein	connexon complex; cellular component	1.18E-24
<i>SSTR4</i>	10.22	somatostatin receptor 4	somatostatin receptor activity; molecular function	4.22E-22
<i>FBN2</i>	9.81	fibrillin 2	binding; molecular function	7.77E-180
<i>HOXC10</i>	8.94	homeobox C10	sequence-specific DNA binding transcription factor activity; molecular function	3.42E-21
<i>DRG1</i>	8.42	developmentally regulated GTP binding protein 1	\	1.73E-18
<i>PLEKHG4</i>	8.33	pleckstrin homology domain containing,	Rho guanyl-nucleotide exchange factor activity; Molecular Function	8.66E-20
<i>RERG</i>	8.21	RAS-like, estrogen-regulated, growth inhibitor	GTPase activity; molecular function	5.57E-19
<i>TBX18</i>	8.15	T-box 18	sequence-specific DNA binding transcription factor activity; molecular function	1.13E-34
<i>IGF2</i>	7.96	insulin-like growth factor 2	hormone activity; molecular function	1.70E-64
Downregulated genes				
<i>SCGB2A2</i>	-15.40	secretoglobin	\	1.56E-134
<i>ORM1</i>	-14.28	orosomucoid 1	regulation of immune system process	2.47E-86
<i>APOC3</i>	-13.92	apolipoprotein C-III	extracellular region; cellular component	1.96E-48
<i>APOB</i>	-13.76	apolipoprotein B	lipid transporter activity; molecular function	8.32E-63
<i>MMP7</i>	-13.68	matrix metalloproteinase 7 (matrilysin, uterine)	etalloendopeptidase activity; molecular function	5.90E-40
<i>SERPINA5</i>	-13.53	serpin peptidase inhibitor	serine-type endopeptidase inhibitor activity; molecular function	9.30E-34
<i>C1QB</i>	-13.33	complement component 1	protein binding; molecular function	1.44E-82
<i>TLR4</i>	-13.07	toll-like receptor	transmembrane receptor activity; molecular function	6.96E-40
<i>SFTPD</i>	-13.02	surfactant protein D	binding; molecular function	1.37E-170
<i>PROX1</i>	-12.28	prospero homeobox 1	DNA binding; molecular function	4.54E-69

Table S2: The top 20 genes with altered expression between the early passages cells (ITH6.1-P9, ITH6.1-P17 and ITH6.1-P24) and the immortalized cells (ITH6.1-P33 and ITH6.1-P47)

Gene name	Log <sub>2</sub> fold change	Description	Functional annotation	<i>P</i> <sub>adj</sub>
Upregulated genes				
<i>ZFX</i>	11.42	zinc finger protein, X-linked	\	2.18E-60
<i>CADPS</i>	11.36	Ca <sup>++</sup> -dependent secretion activator	protein binding; molecular function	5.23E-42
<i>OLFM4</i>	10.37	olfactomedin 4	protein binding; molecular function	9.83E-08
<i>USP9X</i>	10.31	ubiquitin specific peptidase 9	\	2.95E-166
<i>PAX8</i>	9.27	paired box 8	DNA binding; molecular function	5.35E-68
<i>KDM6A</i>	8.15	lysine (K)-specific demethylase 6A	protein binding; molecular function	2.87E-28
<i>KLHL14</i>	7.99	kelch-like 14	protein binding; molecular function, kelch repeat type 1	9.24E-38
<i>MARCH11</i>	7.86	membrane-associated ring finger (C3HC4) 11	\	5.51E-18
<i>CD300E</i>	7.31	CD300e molecule	protein binding; molecular function, immunoglobulin subtype	2.90E-20
<i>EREG</i>	7.28	epiregulin	protein binding; molecular function, ErbB signaling pathway	2.85E-36
Downregulated genes				
<i>KCNB2</i>	-8.53	potassium voltage-gated channel, Shab-related subfamily, member 2	ion channel activity; Molecular Function	2.03E-17
<i>CD34</i>	-8.01	CD34 molecule	cell adhesion; Biological Process	7.70E-11
<i>TMPRSS3</i>	-7.94	transmembrane protease, serine 3	catalytic activity; molecular function	3.37E-17
<i>ARSH</i>	-7.83	arylsulfatase family, member H	catalytic activity; molecular function	7.65E-15
<i>SMOC2</i>	-7.52	SPARC related modular calcium binding 2	calcium ion binding; molecular function	1.49E-45
<i>PLCL1</i>	-7.19	phospholipase C-like 1	phosphoinositide phospholipase c activity; molecular function	1.96E-22
<i>KCNB2</i>	-7.05	potassium voltage-gated channel, Shab-related subfamily, member 2	ion channel activity; molecular function	6.75E-12
<i>RL6</i>	-6.94	ADP-ribosylation factor-like 6 interacting protein 1	endoplasmic reticulum; cellular component	2.62E-32
<i>FAT4</i>	-6.89	FAT tumor suppressor homolog 4 (Drosophila)	calcium ion binding; molecular function	2.95E-13
<i>LMO7</i>	-6.86	LIM domain 7	protein binding; molecular function	2.29E-14